Vol 459|21 May 2009|doi:10.1038/nature08012

LETTERS

Non-genetic origins of cell-to-cell variability in TRAIL-induced apoptosis

Sabrina L. Spencer[1,2]*, Suzanne Gaudet[1]†*, John G. Albeck[1], John M. Burke[1] & Peter K. Sorger[1]

In microorganisms, noise in gene expression gives rise to cell-to-cell variability in protein concentrations[1–7]. In mammalian cells, protein levels also vary[8–10] and individual cells differ widely in their responsiveness to uniform physiological stimuli[11–15]. In the case of apoptosis mediated by TRAIL (tumour necrosis factor (TNF)-related apoptosis-inducing ligand) it is common for some cells in a clonal population to die while others survive—a striking divergence in cell fate. Among cells that die, the time between TRAIL exposure and caspase activation is highly variable. Here we image sister cells expressing reporters of caspase activation and mitochondrial outer membrane permeabilization after exposure to TRAIL. We show that naturally occurring differences in the levels or states of proteins regulating receptor-mediated apoptosis are the primary causes of cell-to-cell variability in the timing and probability of death in human cell lines. Protein state is transmitted from mother to daughter, giving rise to transient heritability in fate, but protein synthesis promotes rapid divergence so that sister cells soon become no more similar to each other than pairs of cells chosen at random. Our results have implications for understanding 'fractional killing' of tumour cells after exposure to chemotherapy, and for variability in mammalian signal transduction in general.

TRAIL elicits a heterogeneous phenotypic response in both sensitive and relatively resistant cell lines: some cells die within 45 min, others 8–12 h later, and yet others live indefinitely (Supplementary Fig. 1). During the variable delay between TRAIL addition and mitochondrial outer membrane permeabilization (MOMP), upstream initiator caspases are active but downstream effector caspases are not[11,12]. Possible sources of cell-to-cell variability in response to TRAIL include genetic or epigenetic differences, stochastic fluctuations in biochemical reactions involving low copy number components ('intrinsic noise'[3]), differences in cell cycle phase, and natural variation in the concentrations of important reactants. To distinguish between these and other possibilities, we used live-cell microscopy to compare the timing and probability of death in sister cells exposed to TRAIL. If phenotypic variability is caused by genetic or epigenetic differences, sister cells should behave identically. In contrast, if stochastic fluctuations in reactions triggered by TRAIL predominate, sister cells should be no more similar to each other than pairs of cells selected at random. The influence of cell cycle state on apoptosis should be readily observable from time-lapse imaging of asynchronous cultures. Furthermore, variability arising from differences in protein levels (or in their activity or modification state) should produce a highly distinctive form of inheritance in which newly born sister cells are very similar, because they inherit similar numbers of abundant factors from their mother[4,7], but then diverge as new proteins are made and levels drift[10,16]. With this in mind, we examined apoptosis in HeLa cells and in non-transformed MCF10A mammary epithelial cells in the presence and absence of protein synthesis inhibitors.

Pairs of sister cells expressing a fluorescent reporter of MOMP (mitochondrial intermembrane space reporter protein, IMS-RP[11]) born during a 20–30 h period were identified by time-lapse microscopy. TRAIL and the protein synthesis inhibitor cycloheximide were then added and imaging continued for another 8 h. The TRAIL-to-MOMP interval (T_d) was calculated for each cell (Fig. 1a). Among the recently divided sisters (<7 h between division and death), T_d was highly correlated ($R^2 = 0.93$, Fig. 1b), whereas T_d was uncorrelated ($R^2 = 0.04$) for recently divided cells chosen at random. The time since division (Fig. 1c) and the position in the dish (data not shown) did not correlate with T_d, ruling out a role for cell cycle state and cell–cell interactions under our experimental conditions. However, as the time since division increased, sister-to-sister correlation in T_d decayed exponentially with a half-life of ~11 h, so that sisters lost memory of shared ancestry within ~50 h or about two cell generations ($R^2 \leq 0.05$, the same as random pairs of cells; Fig. 1d, e). Similar results were obtained with MCF10A cells (Supplementary Fig. 2).

High correlation between recently born sisters shows that the variability in T_d arises from differences that exist before TRAIL exposure, and rules out stochastic fluctuations in signalling reactions. Rapid decorrelation also rules out genetic mutation or conventional epigenetic differences (which typically last $10–10^5$ cell divisions[17]). However, transient heritability is precisely what we expected for cell-to-cell differences arising from variations in the concentrations or states of proteins that are partitioned binomially at cell division.

Whereas all TRAIL-treated HeLa cells eventually died in the presence of cycloheximide, in its absence a fraction always survived (presumably owing to induction of survival pathways[18]). When the fates of sister cells were compared, both lived or both died in most cases (chi-squared test, $P = 7 \times 10^{-19}$, Supplementary Fig. 3). Variability in T_d across the population was large (Fig. 1g and Supplementary Fig. 4), but recently born sisters were nevertheless correlated in T_d ($R^2 = 0.75$, Fig. 1f). Again, cell cycle phase was not correlated with fate or the time-to-death (Fig. 1g). Decorrelation in T_d among sisters was an order of magnitude more rapid in the presence of protein synthesis than in its absence (~1.5 h half-life, Fig. 1h, i and Supplementary Fig. 5). Thus, the length of time that T_d is heritable is very sensitive to rates of protein synthesis, both basal and TRAIL-induced.

We then asked whether the concentrations of proteins regulating TRAIL-induced apoptosis are sufficiently different from cell to cell to account for the variability in T_d. Using flow cytometry, we measured the distributions of five apoptotic regulators for which specific antibodies are available. All five proteins were log-normally distributed across the population with coefficients of variation ranging between 0.21 and 0.28 for cells of similar size (Fig. 2a), consistent with data on

[1]Center for Cell Decision Processes, Department of Systems Biology, Harvard Medical School, Boston, Massachusetts 02115, USA. [2]Computational and Systems Biology, Massachusetts Institute of Technology, Cambridge, Massachusetts 02139, USA. †Present address: Department of Cancer Biology, Dana-Farber Cancer Institute, and Department of Genetics, Harvard Medical School, Boston, Massachusetts 02115, USA.
*These authors contributed equally to this work.

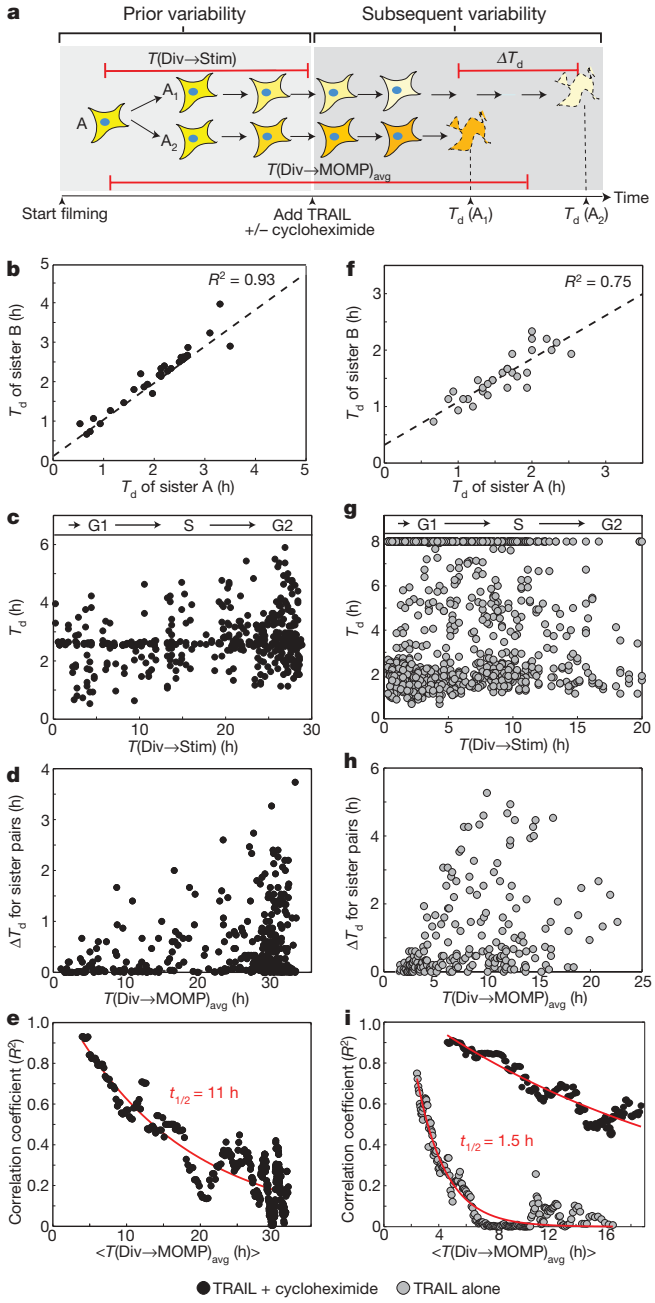

Figure 1 | The time-to-death is highly correlated between HeLa sister cells, but correlation decays as a function of time since division. **a**, Schematic of the experimental design. ΔT_d represents the difference in time of MOMP between sisters; $T(\text{Div}\rightarrow\text{MOMP})_{avg}$ denotes the time between cytokinesis of the mother and the average time of MOMP in daughter cells; $T(\text{Div}\rightarrow\text{Stim})$ denotes the time between cytokinesis and TRAIL addition. The shading of each cell depicts concentrations/states of relevant proteins. **b**, **f**, Similarity in T_d among pairs of recently divided sister cells ($T(\text{Div}\rightarrow\text{MOMP})_{avg} < 7$ h for **b** and < 3.5 h for **f**). **c**, **g**, T_d as a function of $T(\text{Div}\rightarrow\text{Stim})$, a proxy for cell cycle state ($R^2 < 0.03$). **d**, **h**, ΔT_d as a function of $T(\text{Div}\rightarrow\text{MOMP})_{avg}$. **e**, **i**, Decay in the correlation of T_d between sister pairs as a function of $T(\text{Div}\rightarrow\text{MOMP})_{avg}$. In **i**, black circles represent data for cells treated with TRAIL plus cycloheximide, imaged under the same conditions as the TRAIL-alone treatment (Supplementary Fig. 5).

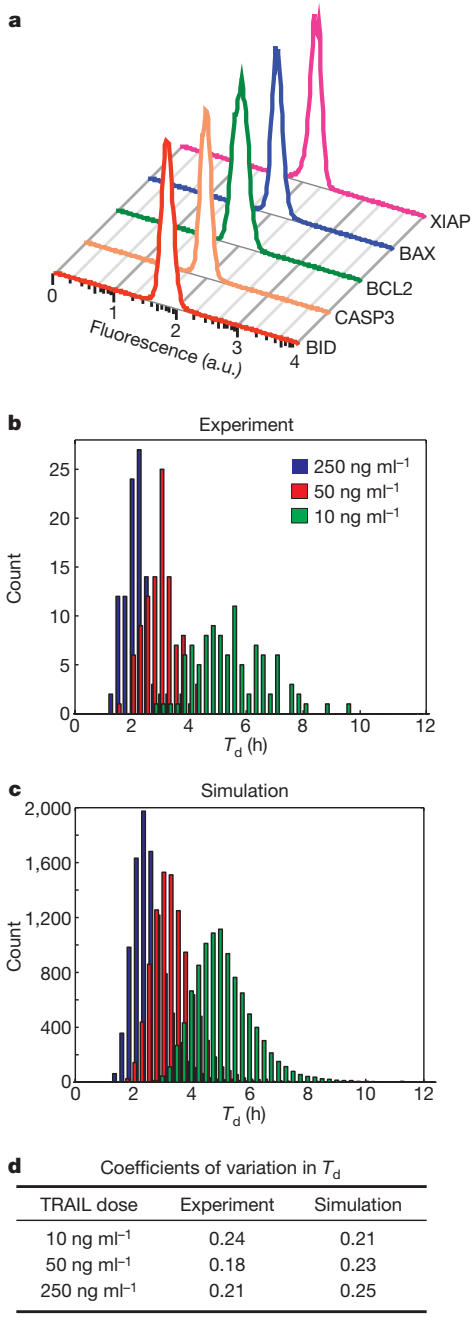

d Coefficients of variation in T_d

TRAIL dose	Experiment	Simulation
10 ng ml^{-1}	0.24	0.21
50 ng ml^{-1}	0.18	0.23
250 ng ml^{-1}	0.21	0.25

Figure 2 | Endogenous variation in the concentrations of apoptotic regulators is sufficient to explain variability in T_d. **a**, Protein distributions in untreated HeLa cells determined by flow cytometry. a.u., arbitrary units. **b**, **c**, Distributions of T_d for HeLa cells treated with TRAIL at concentrations indicated (with cycloheximide) as determined experimentally (**b**) or estimated by simulations (**c**). **d**, Coefficients of variation for distributions in **b** and **c**.

other proteins[10]. To determine the impact of variability in protein levels on variability in time-to-death, we turned to an ordinary differential equation model of TRAIL-induced apoptosis[12]. This model encapsulates the biochemistry of TRAIL-mediated death and recapitulates the dynamics of apoptosis under various conditions of protein depletion or overexpression[12]. When variability in T_d arising from variance in protein levels was modelled, a good match was observed to experimental data (Fig. 2b–d) indicating that the measured differences in protein levels are sufficient to account for variability in T_d.

Next, we investigated which steps in receptor-mediated apoptosis are responsible for variation in time-to-death. To address this question, we grouped reactions into three sets: those occurring before, during, or subsequent to MOMP (Fig. 3a, blue, grey and orange). Before MOMP, TRAIL binds and oligomerizes DR4/5 receptors, promoting assembly of death-inducing signalling complexes (DISCs) that then activate initiator pro-caspases-8 and -10 (CASP8 and CASP10)[19]. Active CASP8/10 cleave BID to a truncated form

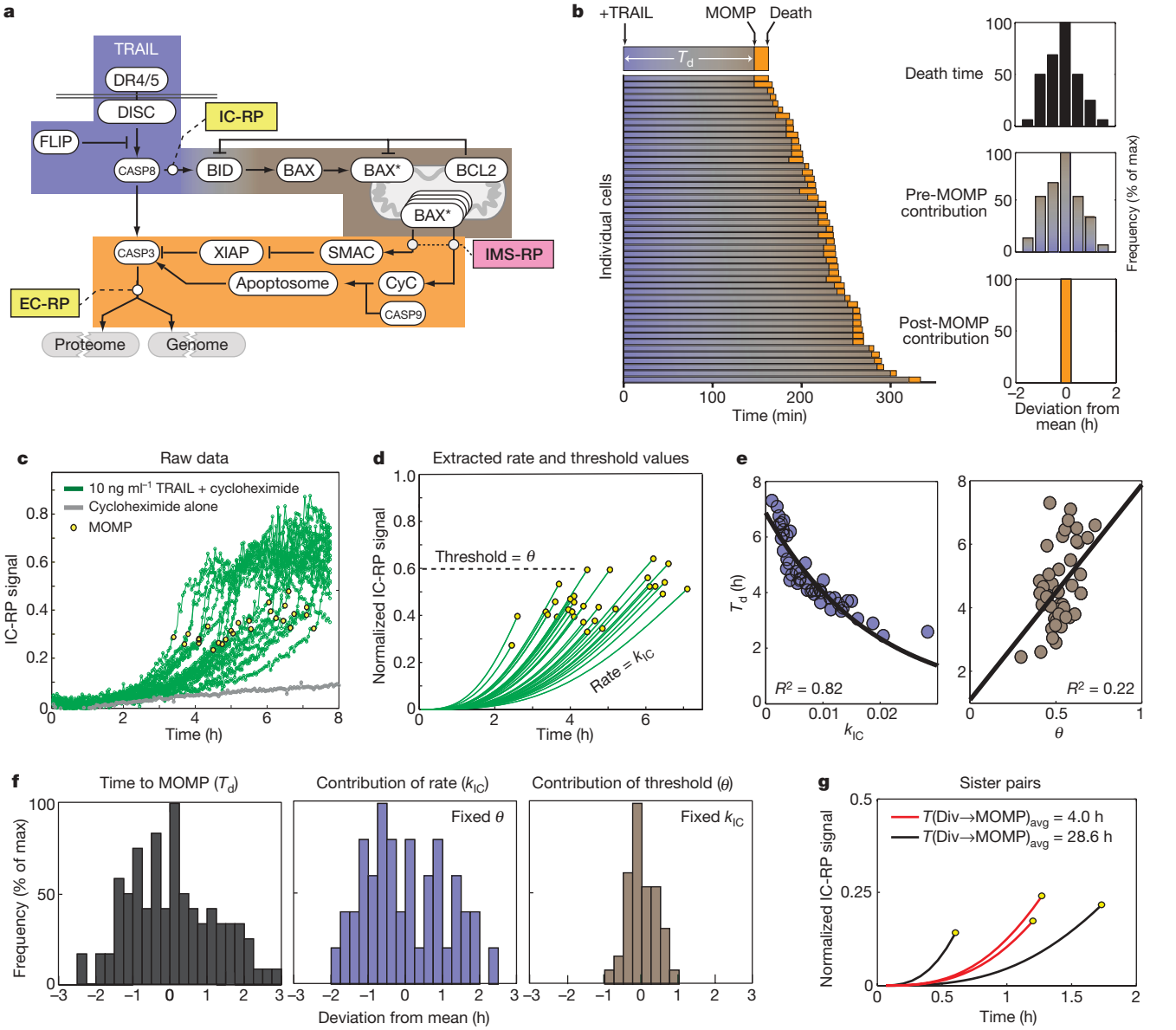

Figure 3 | A single time-dependent process upstream of MOMP predicts the time-to-death. **a**, Schematic of receptor-mediated apoptosis signalling, with IC-RP, EC-RP and IMS-RP indicated. The BCL2 protein family is represented in simplified form by BID, BAX and BCL2. Reactions occur before (blue), during (grey), or subsequent to MOMP (orange). BAX*, activated BAX; CyC, cytochrome *c*. **b**, Timing of apoptotic events in HeLa cells expressing IMS-RP and EC-RP and treated with 50 ng ml^{-1} TRAIL plus cycloheximide; blue-grey denotes the pre-MOMP interval, and orange denotes the interval between MOMP and half-maximal cleavage of EC-RP (a marker of death). Insets show death times computed from data (top) and contributions of pre-MOMP (middle) or post-MOMP (bottom) intervals. **c**, **d**, Raw (**c**) and fitted (**d**) trajectories for IC-RP cleavage in single TRAIL-treated HeLa cells co-expressing IMS-RP and IC-RP. Values for height of the MOMP threshold (θ) and rate of approach to the threshold (k_{IC}) were derived by fitting (Supplementary Fig. 6). **e**, Correlation between T_d and either k_{IC} (left) or θ (right), for data in **d**. **f**, Relative contributions of variability in k_{IC} (blue) or θ (grey) to variability in T_d (black; Supplementary Fig. 7). **g**, Representative trajectories of IC-RP cleavage in recently divided sister HeLa cells having similar T_d (red) and older sisters with differing T_d (black), treated with 50 ng ml^{-1} TRAIL plus cycloheximide.

(tBID)[20,21], which then activates the pore-forming proteins BAX and BAK[22]. CASP8 and CASP10 also process effector pro-caspases-3 and -7 (CASP3 and CASP7), but effector caspase activity is held in check by XIAP until MOMP[19]. MOMP itself involves self-assembly of activated BAX and BAK into transmembrane pores, a process antagonized by anti-apoptotic BCL2 family proteins[22]. When levels of activated tBID, BAX and BAK exceed a threshold set by inhibitory BCL2 proteins, pores form in the mitochondrial outer membrane, allowing cytochrome *c* and SMAC (also known as DIABLO) to translocate into the cytosol[22]. In post-MOMP reactions, cytosolic SMAC neutralizes XIAP, relieving CASP3 and CASP7 inhibition, and allowing cleavage of effector caspase substrates and consequent cell death[19]. In a parallel route to CASP3 and CASP7 activation, cytosolic cytochrome *c* promotes apoptosome assembly and caspase-9 activation.

To establish which steps in TRAIL-induced apoptosis have the greatest impact in determining variability in death time, we imaged cells expressing a reporter protein of either initiator or effector caspase activity (IC-RP or EC-RP)[11] in combination with IMS-RP. We found almost all variability in T_d to arise during the pre-MOMP interval (Fig. 3b). The timing of MOMP itself is determined by the rate at which tBID accumulates to a threshold set by the levels of BCL2 family proteins. This rate and threshold can be inferred from the initial rate of IC-RP cleavage (k_{IC}) and the fraction of IC-RP cleaved (θ) at the time of MOMP, respectively. When k_{IC} and θ were measured in single TRAIL-treated cells, the timing of MOMP was found to be controlled by a variable rate of approach to a threshold of variable height (Fig. 3c, d). However, variation in k_{IC} had a significantly greater role in determining T_d than variation in θ ($R^2 = 0.82$ versus $R^2 = 0.22$;

Fig. 3e, f and Supplementary Fig. 7). Moreover, k_{IC} was very similar in recently born sister cells with similar T_d, but dissimilar in older sisters (Fig. 3g). We conclude that cell-to-cell variability in k_{IC}—and by implication the rate of conversion of BID to tBID—is the primary determinant of variability in the time-to-death under our experimental conditions.

Levels of several proteins set k_{IC}, including DR4/5 receptors, DISC components, CASP8 and BID itself. Modelling suggested that knowing the concentration of any single protein upstream of BID would have minimal value in predicting T_d—the impact of variation in all other proteins is too great (Fig. 4a). Live-cell analysis of FLIP (also known as CFLAR), an important regulator of pro-caspase-8 binding to the DISC, was consistent with this prediction, as was analysis of other single proteins by flow cytometry (Fig. 4b and data not shown). However, modelling showed that with increasing overproduction of BID, measurement of its levels would be increasingly predictive of T_d (Fig. 4c, Supplementary Fig. 8). We therefore measured the relationship between dispersion in T_d and levels of BID tagged with green-fluorescent-protein (GFP) (Fig. 4d). A ~50-fold increase in BID caused the variability in T_d to fall significantly, concomitant with a decrease in mean time-to-death from ~3 h to ~45 min. Thus, only when overexpressed is the level of one protein predictive of T_d; under normal circumstances, control of T_d is multivariate.

Other studies (for example, ref. 23.) address genetic factors determining the average sensitivity of cell lines to TRAIL, whereas this paper examines non-genetic sources of cell-to-cell variability within an individual cell line. We come to three primary conclusions. First, cell-to-cell variation in the timing and probability of death is transiently heritable. Cell cycle state, the number of neighbouring cells, and stochastic fluctuations in TRAIL-induced signalling reactions do not have a crucial involvement under our conditions. Instead, variability in phenotype arises from cell-to-cell differences in protein levels that exist before TRAIL exposure (our experiments do not distinguish between cell-to-cell differences in total concentrations and in post-translationally modified forms). Second, the rate at which sisters lose memory of a shared past is an order of magnitude faster in the presence of protein translation than in its absence. This further implicates variability in protein levels as the origin of differences in phenotype. Third, knowing the concentration of individual proteins does not allow T_d to be predicted, but measuring the rate of a single reaction does (BID to tBID conversion in our experiments). This finding probably holds for other examples of ligand-induced apoptosis; however for intrinsic apoptosis, different proteins will control the rate of approach to MOMP and θ may dominate in certain contexts. The fundamental point is that each of these properties is determined by the levels and activities of several proteins. Given the prevalence of multi-protein cascades in signal transduction, multivariate control over cell-to-cell variability is likely to be more common than the univariate control observed in other settings[8,23,24].

Heritable, non-genetic determinants of phenotype are often referred to as 'epigenetic'[17], but the transient heritability we observe here is fundamentally different in origin and duration. Given variability in growth rates and noise in gene expression, genetically identical cells will inevitably contain slightly different concentrations of most proteins. However, differences in protein concentrations do not necessarily affect phenotype, a property often referred to as robustness[25]. For example, the efficiency with which effector caspase substrates are cleaved does not vary much from cell to cell[12]. Given the importance of tight control over apoptosis, cell-to-cell variability in the timing and probability of death seems unlikely to reflect an inability of cells to achieve robust regulation. Instead, by transforming what is a binary decision at the single-cell level into a graded response at the population level, variability probably has an adaptive advantage.

TRAIL is at present undergoing clinical trials as an anti-cancer drug[26] and our findings may have implications for the use of TRAIL and other apoptosis inducers as therapeutics. Many drugs exhibit 'fractional killing', in which each round of therapy kills some but not all of the cells in a tumour[27]. Traditionally, this is thought to reflect differences in genotype, cell cycle state, or the involvement of

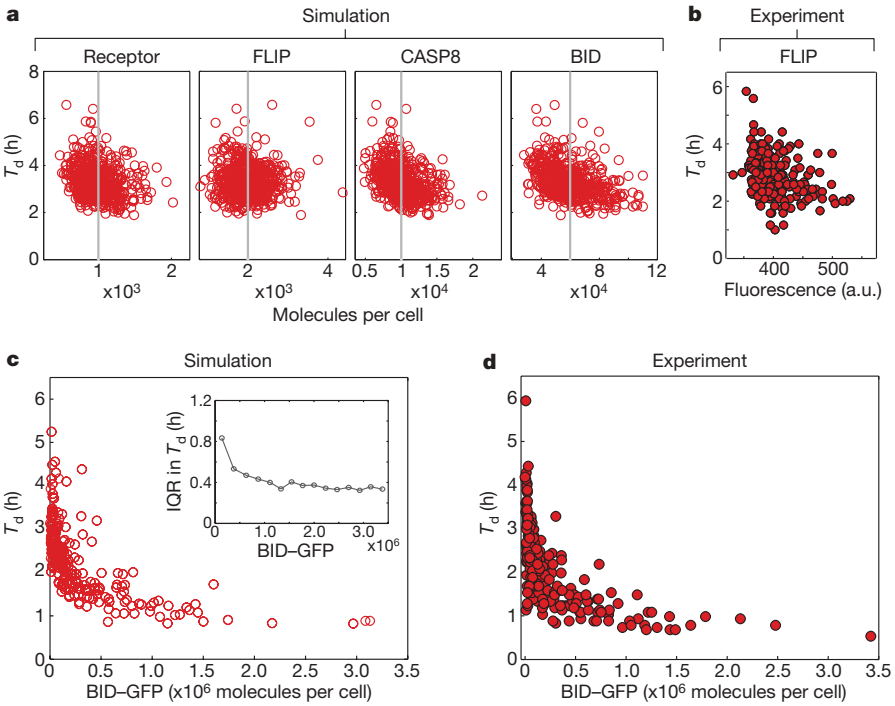

Figure 4 | No single protein predicts T_d under normal conditions but overexpression can increase predictability. **a**, T_d as a function of four protein levels, based on simulation as in Fig. 2c. Grey lines denote mean protein concentration; each point represents a single simulated cell. **b**, Death time as a function of endogenous FLIP levels in H1299 cells. **c**, **d**, Effect of BID–GFP overexpression on T_d in HeLa cells, as predicted by simulation (**c**) or observed in experiment (**d**). Inset shows the reduction in dispersion of T_d with increasing BID–GFP, as measured by the interquartile range (IQR; Supplementary Fig. 8).

cancer stem cells, but our data demonstrate that marked variability can also arise from natural differences in protein levels. We propose that the efficiency of TRAIL-mediated killing of cancer cells could be increased by reducing the impact of cell-to-cell variability, perhaps through co-drugging.

METHODS SUMMARY

Live-cell microscopy. Cells expressing IMS-RP and Förster resonance energy transfer (FRET) reporters EC-RP or IC-RP were imaged as described[11]. In Fig. 1, cells were imaged for 20–30 h to determine the time of division and to identify sister pairs; media containing 50 ng ml^{-1} TRAIL plus 2.5 μg ml^{-1} cycloheximide, or 250 ng ml^{-1} TRAIL alone, was then added. The difference in TRAIL concentrations was designed to generate a similar range in T_d with and without cycloheximide (Supplementary Fig. 4). Cells were then imaged for 8 h to determine the time of MOMP, by monitoring cytosolic translocation of IMS-RP. Unless otherwise noted, all treatments included 2.5 μg ml^{-1} cycloheximide.

Data analysis. Correlation coefficients (R^2) were obtained by linear regression except where noted. Sister–sister correlation was determined by sorting pairs of cells on $T(\mathrm{Div}\rightarrow\mathrm{MOMP})_{\mathrm{avg}}$ (where 'Div' denotes division) and calculating R^2 for the first 40 pairs. R^2 was then recalculated for cells 2–41, 3–42, and so on, and the results were plotted as a function of the average $T(\mathrm{Div}\rightarrow\mathrm{MOMP})_{\mathrm{avg}}$ for the 40 cells in question, denoted by '$<\ >$'. The results were fit to an exponential decay $R^2 = 1.2e^{(-0.063\ T(\mathrm{Div}\rightarrow\mathrm{MOMP})_{\mathrm{avg}})}$ for TRAIL plus cycloheximide, and $R^2 = 2.3e^{(-0.47T(\mathrm{Div}\rightarrow\mathrm{MOMP})_{\mathrm{avg}})}$ for TRAIL alone. Half-lives were calculated as $\ln(2)/0.063 = 11$ h, and $\ln(2)/0.47 = 1.5$ h. Contributions to T_d of k_{IC}, θ and pre- and post-MOMP intervals were obtained by fixing one parameter at the mean value and allowing the other to vary over the observed range, then mean-centring the resulting distributions (Supplementary Fig. 7). Fitted IC-RP trajectories were obtained after subtracting a trajectory for cycloheximide alone (Fig. 3c) to control for photobleaching (Supplementary Fig. 6).

Modelling. The responses of cell populations were simulated using a trained ordinary differential equation model[12] sampling from log-normally distributed protein concentrations with coefficient of variation (CV) ≈ 0.25 (see Methods). In Fig. 4, BID–GFP (an experimental observable) was added to log-normally distributed endogenous BID (unobservable); other proteins were sampled from log-normal distributions as before. Simulations were adjusted to match the distribution BID–GFP achieved experimentally.

Full Methods and any associated references are available in the online version of the paper at www.nature.com/nature.

Received 7 March; accepted 25 March 2009.
Published online 12 April 2009.

1. Blake, W. J., Kærn, M., Cantor, C. R. & Collins, J. J. Noise in eukaryotic gene expression. *Nature* **422,** 633–637 (2003).
2. Colman-Lerner, A. *et al.* Regulated cell-to-cell variation in a cell-fate decision system. *Nature* **437,** 699–706 (2005).
3. Elowitz, M. B., Levine, A. J., Siggia, E. D. & Swain, P. S. Stochastic gene expression in a single cell. *Science* **297,** 1183–1186 (2002).
4. Golding, I., Paulsson, J., Zawilski, S. M. & Cox, E. C. Real-time kinetics of gene activity in individual vacteria *Cell* **123,** 1025–1036 (2005).
5. McAdams, H. H. & Arkin, A. Stochastic mechanisms in gene expression. *Proc. Natl Acad. Sci. USA* **94,** 814–819 (1997).
6. Ozbudak, E. M., Thattai, M., Kurtser, I., Grossman, A. D. & van Oudenaarden, A. Regulation of noise in the expression of a single gene. *Nature Genet.* **31,** 69–73 (2002).
7. Rosenfeld, N., Young, J. W., Alon, U., Swain, P. S. & Elowitz, M. B. Gene regulation at the single-cell level. *Science* **307,** 1962–1965 (2005).
8. Chang, H. H., Hemberg, M., Barahona, M., Ingber, D. E. & Huang, S. Transcriptome-wide noise controls lineage choice in mammalian progenitor cells. *Nature* **453,** 544–547 (2008).
9. Feinerman, O., Veiga, J., Dorfman, J. R., Germain, R. N. & Altan-Bonnet, G. Variability and robustness in T cell activation from regulated heterogeneity in protein levels. *Science*, **321,** 1081–1084 (2008).
10. Sigal, A. *et al.* Variability and memory of protein levels in human cells. *Nature* **444,** 643–646 (2006).
11. Albeck, J. G. *et al.* Quantitative analysis of pathways controlling extrinsic apoptosis in single cells. *Mol. Cell* **30,** 11–25 (2008).
12. Albeck, J. G., Burke, J. M., Spencer, S. L., Lauffenburger, D. A. & Sorger, P. K. Modeling a snap-action, variable-delay switch controlling extrinsic cell death. *PLoS Biol.* **6,** 2831 (2008).
13. Geva-Zatorsky, N. *et al.* Oscillations and variability in the p53 system. *Mol. Syst. Biol.* **2,** 2006.0033 (2006).
14. Goldstein, J. C., Kluck, R. M. & Green, D. R. A single cell analysis of apoptosis. Ordering the apoptotic phenotype. *Ann. NY Acad. Sci.* **926,** 132–141 (2000).
15. Lahav, G. *et al.* Dynamics of the p53–Mdm2 feedback loop in individual cells. *Nature Genet.* **36,** 147–150 (2004).
16. Kaufmann, B. B., Yang, Q., Mettetal, J. T. & van Oudenaarden, A. Heritable stochastic switching revealed by single-cell genealogy. *PLoS Biol.* **5,** e239 (2007).
17. Rando, O. J. & Verstrepen, K. J. Timescales of genetic and epigenetic inheritance. *Cell* **128,** 655–668 (2007).
18. Chaudhary, P. M., Eby, M., Jasmin, A., Bookwalter, A., Murray, J. & Hood, L. Death receptor 5, a new member of the TNFR family, and DR4 induce FADD-dependent apoptosis and activate the NF-κB pathway. *Immunity* **7,** 821–830 (1997).
19. Fuentes-Prior, P. & Salvesen, G. S. The protein structures that shape caspase activity, specificity, activation and inhibition. *Biochem. J.* **384,** 201–232 (2004).
20. Li, H., Zhu, H., Xu, C. & Yuan, J. Cleavage of BID by caspase 8 mediates the mitochondrial damage in the Fas pathway of apoptosis. *Cell* **94,** 491–501 (1998).
21. Luo, X., Budihardjo, I., Zou, H., Slaughter, C. & Wang, X. Bid, a Bcl2 interacting protein, mediates cytochrome c release from mitochondria in response to activation of cell surface death receptors. *Cell* **94,** 481–490 (1998).
22. Youle, R. J. & Strasser, A. The BCL-2 protein family: opposing activities that mediate cell death. *Nature Rev. Mol. Cell Biol.* **9,** 47–59 (2008).
23. Wagner, K. W. *et al.* Death-receptor O-glycosylation controls tumor-cell sensitivity to the proapoptotic ligand Apo2L/TRAIL. *Nature Med.* **13,** 1070–1077 (2007).
24. Cohen, A. A. *et al.* Dynamic proteomics of individual cancer cells in response to a drug. *Science*, **322,** 1511–1516 (2008).
25. Barkai, N. & Leibler, S. Robustness in simple biochemical networks. *Nature* **387,** 913–917 (1997).
26. Ashkenazi, A. & Herbst, R. S. To kill a tumor cell: the potential of proapoptotic receptor agonists. *J. Clin. Invest.* **118,** 1979–1990 (2008).
27. Berenbaum, M. C. *In vivo* determination of the fractional kill of human tumor cells by chemotherapeutic agents. *Cancer Chemother. Rep.* **56,** 563–571 (1972).

Supplementary Information is linked to the online version of the paper at www.nature.com/nature.

Acknowledgements We thank D. Flusberg, S. Govind, L. Kleiman, A. Letai, B. Millard, R. Milo, T. Norman, J. Paulsson and R. Ward for their help. This work was supported by National Institute of Health (NIH grants) GM68762 and CA112967.

Author Information Reprints and permissions information is available at www.nature.com/reprints. The authors declare competing financial interests: details accompany the full-text HTML version of the paper at www.nature.com/nature. Correspondence and requests for materials should be addressed to P.K.S. (peter_sorger@hms.harvard.edu).

METHODS

Cell culture and transfections. HeLa cells were maintained in DMEM (Mediatech, Inc.) supplemented with L-glutamine (Gibco), penicillin/streptomycin (Gibco) and 10% fetal bovine serum (FBS; Mediatech, Inc.). MCF10A cells were cultured as described[28]. H1299 cells containing FLIP tagged with yellow fluorescent protein (YFP) at the endogenous locus were obtained from the Kahn Dynamic Proteomics Project and maintained at 8% CO_2 in RPMI (Mediatech, Inc.) with 10% FBS and penicillin/streptomycin. HeLa cells expressing IMS-RP[11] were transfected using FuGENE 6 (Roche) with pd4-BID-EGFP (Clontech) to sample expression levels across a wide range. H1666 cells were maintained (and imaged) in RPMI supplemented with 10% FBS, L-glutamine, penicillin/streptomycin, 1× ITES (Lonza Biosciences), 50 nM hydrocortisone, 10 μM phosphorylethanolamine, 0.1 nM Tri-iodothyronine, 10 mM HEPES, 0.5 mM sodium pyruvate, 2 g l^{-1} BSA and 1 ng ml^{-1} EGF. Fresh primary liver cells were obtained from CellzDirect and plated on collagen type I. Cells were maintained (and imaged) in Eagle's Minimum Essential Medium supplemented with 10% FBS, L-glutamine, 100 nM dexamethasone, 5 μg ml^{-1} human insulin, 5 μg ml^{-1} transferrin from human serum, 5 μg ml^{-1} sodium selenite and 15 mM HEPES. SKBR3 cells were maintained (and imaged) in RPMI supplemented with 10% FBS, L-glutamine and penicillin/streptomycin.

Live-cell microscopy. HeLa cells expressing IMS-RP and FRET reporters EC-RP or IC-RP were imaged in a 37 °C humidified chamber as described[11]. For sister cell experiments, HeLa cells expressing IMS-RP were imaged[11] at 10-min intervals for 20–30 h in phenol-red-free CO_2-independent medium (Invitrogen) with L-glutamine, penicillin/streptomycin and 1% serum (Fig. 1b–e), or at ~5% CO_2 in phenol-red-free DMEM with L-glutamine, penicillin/streptomycin and 10% serum (Fig. 1f–i, see also Supplementary Fig. 5). The growth media was then replaced with the same media containing TRAIL (Alexis Biochemicals), with or without 2.5 μg ml^{-1} cycloheximide (Sigma-Aldrich), and images were acquired at 3-min intervals for an additional 8 h. Cells still alive at the end of the 8 h were considered to have survived the treatment. MFC10A were imaged as described[11] but at ~5% CO_2 in phenol-red-free assay media[28] without EGF or insulin, to reduce cell migration. HeLa cells co-expressing IMS-RP and BID–GFP and H1299 FLIP–YFP cells were imaged[11] in the same media as described earlier for Fig. 1b–e but at ×20 magnification with frames every 3 or 10 min, respectively. H1666, SKBR3 and primary liver cells were imaged in 96-well glass bottom plates (Matrical) on a Nikon TE2000E at ×10 magnification in a 37 °C chamber with 5% CO_2.

Image analysis. Sister-cell tracking was performed manually. To assess whether there is a cell cycle effect on death time, we plotted death time as a function of time since division, as a proxy for cell cycle phase. Because the distribution of time since division is not uniform, one might infer a cell cycle effect but, in fact, a cell cycle effect would appear as a slope in the data, which we do not observe. For sister cell experiments in which CO_2-independent medium was used, there was more proliferation early in the sister-cell tracking movie (and thus more points near 'G2') because CO_2-independent medium does not support very long-term proliferation (division slows down, but the cells are not dying). Notably, the lack of a cell cycle effect is also apparent for sister cell experiments performed in DMEM—the standard medium for HeLa cells (Supplementary Fig. 5). In these experiments, the cells proliferated continuously during the sister-cell tracking movie. Cells that divided early in the movie often divided again if they survived stimulation with TRAIL, producing 'cousins' that were excluded from the analysis. This resulted in fewer cells in the G2 region, but this does not indicate a cell cycle effect, as the probability of surviving or dying is constant.

Analysis of IC-RP and EC-RP cleavage and IMS-RP translocation was performed as described[11]. To derive estimates for k_{IC} and θ, individual cell trajectories were fit with an equation derived from mathematical reduction of the differential equation model for the pathway (J.M.B., J.G.A, S.L.S., D. Lauffenburger and P.K.S., manuscript in preparation; see also Supplementary Fig. 5). The equations for the fitted relationship between T_d and k_{IC} and between T_d and θ were: $T_d = 6.9e^{(-53.7k_{IC})}$ and $T_d = 6.8\ \theta + 1.1$. FLIP–YFP fluorescence was quantified at $t = 0$ h (time of TRAIL addition) by manually outlining the cell and measuring the average fluorescence intensity within the outline. For FLIP–YFP cells, the time of death was scored as the first frame in which a cell exhibited apoptotic morphology. The slight pro-apoptotic effect observed with FLIP levels could be owing to its role as an activator of initiator caspases at low FLIP/CASP8 ratios[29]. BID–GFP fluorescence was quantified at $t = 0$ h by measuring the average fluorescence intensity from a representative area within the cell. To determine the absolute number of proteins per cell, the average BID–GFP fluorescence intensity from these movies was set equal to the average number of GFP-tagged proteins per cell as measured by quantitative immunoblot (Supplementary Fig. 9).

Flow cytometry. The distributions of initial protein levels were measured in HeLa cells (fixed with paraformaldehyde and permeabilized with methanol) on a FACSCalibur (BD Biosciences). The antibodies were carefully validated by knockout or knockdown and/or by overexpression of GFP-tagged fusion proteins. The following antibodies were used: anti-BID (HPA000722, Atlas Antibodies), anti-BAX (MAB4601, Chemicon International), anti-BCL2 (SC7382, Santa Cruz Biotechnology), anti-XIAP (610717, BD Biosciences) and anti-CASP3 (SC7272, Santa Cruz Biotechnology).The coefficient of variation of cells of similar size (as estimated by forward scatter) ranged from 0.21 to 0.28.

Modelling. The details of methods used will be described elsewhere (S.G., S.L.S., W. W. Chen and P.K.S., manuscript in preparation). In brief, a series of 10^4 simulations of the EARMv1.1 ordinary differential equation model[12] (modified to include general protein synthesis and degradation) were run in Jacobian (Numerica Technology). In previous work, only single values for each protein concentration were used[12]. Here, for each run of the model (representing one cell), initial protein levels were independently sampled from log-normal distributions having mean values as listed in Supplementary Table 1, and coefficients of variation as measured by flow cytometry (Fig. 2a) or set to 0.25 for proteins that were not measured. Initial protein concentrations and parameter values are listed in Supplementary Tables 1 and 2.

28. Debnath, J., Muthuswamy, S. K. & Brugge, J. S. Morphogenesis and oncogenesis of MCF-10A mammary epithelial acini grown in three-dimensional basement membrane cultures. *Methods* **30**, 256–268 (2003).
29. Boatright, K. M., Deis, C., Denault, J. B., Sutherlin, D. P. & Salvesen, G. S. Activation of caspases-8 and -10 by $FLIP_L$. *Biochemical journal* **382**, 651–657 (2004).